Ecological Indicators 112 (2020) 106153

Contents lists available at ScienceDirect

Ecological Indicators

journal homepage: www.elsevier.com/locate/ecolind

Application conditions and impact factors for various vegetation indices in constructing the LAI seasonal trajectory over different vegetation types

Kun Qiao[a,b], Wenquan Zhu[a,b,*], Zhiying Xie[a,b]

[a] State Key Laboratory of Earth Surface Processes and Resource Ecology, Beijing Normal University, Beijing 100875, China
[b] Beijing Engineering Research Center for Global Land Remote Sensing Products, Institute of Remote Sensing Science and Engineering, Faculty of Geographical Science, Beijing Normal University, Beijing 100875, China

ARTICLE INFO

Keywords:
Leaf area index
Vegetation indices
Whole growing season
Red-edge
Vegetation types
Global sensitivity analysis

ABSTRACT

Leaf area index (LAI) is a required input for various ecological and crop models. To investigate the application conditions of various vegetation indices (VIs), especially the VIs constructed by red-edge band (VI_{RE}) for estimating LAI, six VIs derived from Medium Resolution Imaging Spectrometer (MERIS) data were used to construct LAI seasonal trajectory for different vegetation types at 15 sites. The PROSAIL model combined with the Extended Fourier Amplitude Sensitivity Test (EFAST) method was adopted to explore the influences and physical basis of canopy biophysical and non-canopy variables on the construction of LAI seasonal trajectory using VIs. For deciduous forests, the normalized difference vegetation index (NDVI) had the highest sensitivity to LAI when LAI $<$ 2, while the RE normalized difference vegetation index (NDVIRE) had the highest sensitivity when LAI $>$ 2. For evergreen forests, there were no obvious differences among the sensitivities of six VIs to LAI when LAI $<$ 5, while the RE chlorophyll index (CIRE) had the highest sensitivities when LAI $>$ 5. For crops, all the VIs had the similar sensitivities at LAI $<$ 3, while the CIRE and MERIS terrestrial chlorophyll index (MTCI) were most sensitive to LAI variations at LAI $>$ 3. For all three types of vegetation, the VI_{RE} maintained relatively high sensitivity to LAI over the whole range of LAI, especially at high LAI values. The VIs were most affected by chlorophyll content (Cab) and average leaf inclination angle (ALA); their total contribution was about 85%. However, the influence of ALA on VI_{RE} was relatively weak, implying that the VI_{RE} had the potential to establish a universal model for LAI estimation among different vegetation types. Therefore, the optimal VIs over different ranges of LAI were suggested to estimate LAI. In addition, the VI_{RE} should be a preferred choice for estimating LAI to reduce the simulation errors of seasonal LAI, if the RE band is available.

1. Introduction

Leaf area index (LAI) is usually defined as half the total green leaf area per unit ground surface area (Chen and Black, 1992). It is one of the representative vegetation biophysical parameters and the essential climate variables (ECVs) (Brown et al., 2017). As a required input for various terrestrial ecological and crop growth models, LAI is critical for crop yield estimation, forest monitoring, ecological assessment and carbon cycle research (Battaglia et al., 2004; Casa et al., 2012; Richardson et al., 2011; Shang et al., 2014). LAI is a core canopy structural variable that reflects the seasonal status of the vegetation growth, and characterizes the canopy interception area of light and water. In addition, it is also a key indicator that closely relates to various biophysical processes of the vegetation, including the processes of evapotranspiration, respiration, photosynthesis and carbon or nitrogen cycles (Garrigues et al., 2008; Tian et al., 2017; Viña et al., 2011; Xu et al., 2018).

Currently, there are two main types of methods for LAI estimation using remote sensing data: (1) statistical relationships between LAI and spectral vegetation indices (VIs), and (2) vegetation radiative transfer models (Atzberger et al., 2015; Campos-Taberner et al., 2016; Yan et al., 2019). VI is the mathematical combination of different spectral bands based on the absorption and reflection characteristics of vegetation. It is able to minimize the non-vegetation signals, thereby enhancing the vegetation information contained in spectral reflectance data. Thus, VI is commonly used for monitoring the variability of the vegetation characteristics (e.g., LAI) (Moulin, 1999; Viña et al., 2011). Many studies successfully related VIs to LAI in various vegetation types, such as grasslands, crops, deciduous forests and evergreen forests (Atzberger et al., 2015; Delegido et al., 2013; Din et al., 2017; Korhonen

* Corresponding author at: Beijing Normal University, No. 19, Xinjiekouwai St, Haidian District, Beijing 100875, China.
E-mail address: zhuwq75@bnu.edu.cn (W. Zhu).

https://doi.org/10.1016/j.ecolind.2020.106153
Received 23 October 2019; Received in revised form 14 January 2020; Accepted 29 January 2020
Available online 06 February 2020
1470-160X/

et al., 2017; Kross et al., 2015; Nguy-Robertson et al., 2014). The normalized difference vegetation index (NDVI) is the most widely used VI for LAI estimation, but it is susceptible to the soil reflectance when LAI values are relatively low, and its sensitivity decreases rapidly with the increase of LAI (Gu et al., 2013). Some improved VIs, such as enhanced vegetation index (EVI), perpendicular vegetation index (PVI) and atmospherically resistant vegetation index (ARVI) were therefore developed to reduce the influences from soil background reflectance and other factors. However, the saturation of the VIs at high LAI values still exists. Besides, the LAI estimation models established by these improved VIs are less generic (Birky, 2001; Cheng et al., 2003; Gu et al., 2013).

Recently, the VIs constructed by the red edge band (VI_{RE}) were found to be effective in overcoming the saturation problem at high LAI values. In addition, they were less affected by canopy structures. Therefore, they have potential to develop a universal model for estimating LAI (Eitel et al., 2011; Nguy-Robertson et al., 2014; Schuster et al., 2012). However, most of these studies were based on the data in a single vegetation type or a single phenological period, lacking a comprehensive analysis for the application conditions of various VIs (including VI_{RE}) in LAI estimation in the whole growing season for different vegetation types. Besides, most studies utilized the simulated red-edge band reflectance for analysis (Nguy-Robertson and Gitelson, 2015; Viña et al., 2011). Furthermore, the LAI-VI relationship is determined by a variety of factors, including leaf properties (e.g., chlorophyll content, water content and dry matter content), canopy structures (e.g., leaf inclination angle distribution and clumping index), soil background properties, and sun-sensor geometry and illumination conditions (e.g., hotspot and solar zenith angle) (Liu et al., 2012; Xie et al., 2018). The uncertainties in LAI-VI relationship increase due to the compounded influence of these factors. Thus, it is need to quantitatively evaluate the contributions and impact mechanism of relevant impact factors, especially how these factors affect the performances of VI_{RE}. The types of relationships between LAI and VIs are also diverse, including linear, quadratic polynomial, cubic polynomial and logarithmic relationships (le Maire et al., 2011; Li et al., 2016; Potithep et al., 2013). To clearly understand the responses of various VIs to LAI, and further to obtain a more stable LAI-VI relationship and the optimal VI in constructing the LAI seasonal trajectory, it is necessary to analyze the LAI-VI relationships for different vegetation types using multi-year and multi-site data.

In this study, continuous LAI observation data and six VIs calculated from Medium Resolution Imaging Spectrometer (MERIS) data were used to evaluate the performances of VIs in constructing the LAI seasonal trajectory for different vegetation types. The specific objectives of this study are (1) to investigate the application conditions for various VIs in constructing the LAI seasonal trajectory for different vegetation types; (2) to compare the performances of VIs constructed by the green, red and red-edge bands, revealing the possible advantages of VI_{RE} in LAI estimation; and (3) to quantitatively assess the impact factors for LAI-VI relationship, and investigate the physical basis of LAI estimation using VIs and the feasibility of building a universal LAI estimation model.

2. Material and methodology

2.1. Sites and data acquisition

2.1.1. Ground LAI data

Considering the availability of at least 3 years of ground-observed LAI data within the operational period of MERIS, 15 study sites were selected from database of AmeriFlux, Japan Long Term Ecological Research Network and Chinese Ecosystem Research Network (Table 1). These study sites are dominated by deciduous forest, evergreen forest and crop. Their LAI data were measured in plots in fields of vegetation every 10 to 30 days from the start of the growing season (SGS) to the end of the growing season (EGS).

2.1.2. MERIS data and preprocessing

MERIS level 2 full-resolution full-swath (MER_FRS_2P) data were used for VI calculation. They were obtained from the data website of European Space Agency (https://earth.esa.int/). MER_FRS_2P data contain 13 spectral bands of bottom-of-atmosphere (BOA) reflectance with a spatial resolution of 300 m and a quality layer. And its temporal resolution is 3 days. The BOA reflectance values of each band are the results of a partial atmospheric correction, eliminating the influences of gaseous absorption and Rayleigh scattering. The spectral range of the 13 bands covers the visible to near-infrared (NIR) region, including a red-edge band.

Some preliminary data processing such as geometric correction and reprojection were carried out using ESA's Sentinel Application Platform (ESA-snap). To ensure the spatial consistency of the LAI and MERIS VI data, the mean value of 9 pixels within the 3 × 3 window was extracted centered on the pixel corresponding to each site, except for where cloud was present according to the quality layer and visual interpretation. In addition, a time-weighted linear interpolation was applied for VI data to ensure the temporal consistent with LAI data (Viña et al. 2011).

2.2. Methodology

2.2.1. Calculations of spectral VIs

Six VIs, including NDVI, red edge normalized difference vegetation index (NDVIRE), green normalized difference vegetation index (NDVIgreen), MERIS terrestrial chlorophyll index (MTCI), red edge chlorophyll index (CIRE) and green chlorophyll index (CIgreen), were calculated from MERIS reflectance data (Table 2). The bands used to compute VIs include the green band: b5 (555–565 nm), red band: b8 (677.5–685 nm), red-edge band: b9 (703.75–713.75 nm), and near-infrared band: b10 (750–757.5 nm) and b12 (771.25–786.25 nm).

2.2.2. Performance evaluations of VIs in constructing LAI seasonal trajectory

The SPSS software (version 20.0) was utilized to evaluate the performances of VIs in constructing LAI seasonal trajectory. Firstly, the quadratic polynomial model was selected for fitting the LAI-VI relationships at the sites after some initial tries, and to evaluate the performances of VIs in constructing LAI seasonal trajectory at sites. Then the multi-site LAI and VI data for the same vegetation type were pooled together to evaluate the performances of VIs in constructing LAI seasonal trajectory for different vegetation types (the data for deciduous forests only included data from four sites: US-Ha1-EMS, US-Ha1-LPH, US-UMB and US-MMS, because the geographic locations of CA-Oas and JP-Tak sites are too far away from those four sites, besides, the meteorological conditions and tree species of these two sites are completely different from others); and the linear and quadratic polynomial models were selected for fitting the LAI-VI relationships for different vegetation types. The coefficient of determination (R^2) and root mean square error (RMSE) for these models were calculated simultaneously.

A paired T-test was conducted for the LAI-VI regressions at the sites to examine whether there were significant differences in the performances of various VIs in constructing LAI seasonal trajectory for multiple sites. In addition, an F-test was performed to examine whether there were significant LAI-VI regressions in the models.

2.2.3. Sensitivities analysis of VIs against LAI

The sensitivities of different spectral VIs against LAI changes were assessed by the Noise Equivalent ΔLAI of the LAI-VI relationships (Equation (1)). The higher the *NEΔLAI* value is, the lower the sensitivity is (Viña et al., 2011; Xie et al., 2018).

$$NE\Delta LAI = \frac{RMSE\{VI\ vs.\ LAI\}}{d(VI)/d(LAI)} \quad (1)$$

where RMSE and d(VI)/d(LAI) are, respectively, the root mean square error and the first derivative of the best-fit function in the relationship

Table 1
Descriptions of study sites.

Site ID	Study site	Country	Longitude	Latitude	Elevation (m)	Dominant vegetation	Measurement interval (years)
US-Ha1-EMS	Harvard forest	USA	−72.171	42.538	340	DF	2006–2011
US-Ha1-LPH	Harvard forest	USA	−72.183	42.541	340	DF	2007–2010
US-UMB	University of michigan biological station	USA	−84.714	45.560	243	DF	2003–2011
US-MMS	Morgan monroe state forest	USA	−86.413	39.323	275	DF	2003–2006
CA-Oas	SSA Old aspen	Canada	−106.200	53.63	601	DF	2002–2004
JP-Tak	Takayama	Japan	137.423	36.146	1420	DF	2007–2008, 2010–2011
CN-XSBN1	Xishuangbanna tropical monsoon forest	China	101.200	21.961	750	EF	2005–2011
CN-XSBN2	Xishuangbanna tropical artificial rubber forest	China	101.274	21.911	580	EF	2005–2011
CN-XSBN3	Xishuangbanna tropical artificial rainforest	China	101.268	21.922	570	EF	2005–2011
CN-XSBN4	Xishuangbanna karst monsoon forest	China	101.283	21.912	640	EF	2005–2011
CN-HT1	Huitong broad-leaved evergreen forests	China	109.608	26.843	358	EF	2007–2008, 2010–2011
CN-HT2	Huitong chinese fir plantation	China	109.605	26.851	520	EF	2007–2008, 2010–2011
US-Ne1	Mead-irrigated continuous maize site	USA	−96.476	41.165	361	CRO	2003–2007
US-Ne2	Mead-irrigated maize-soybean rotation site	USA	−96.470	41.165	362	CRO	2003–2007
US-Ne3	Mead-rainfed maize-soybean rotation site	USA	−96.440	41.180	363	CRO	2003–2007

DF: Deciduous forest; EF: Evergreen forest; CRO: Crop.

"VI vs. LAI".

2.2.4. Radiative transfer modelling and global sensitivity analysis

To investigate the influences of canopy biophysical parameters, soil parameters and other environmental parameters on the construction of LAI seasonal trajectory with VIs, PROSAIL model was utilized to simulate the spectral reflectance to calculate six VIs. Firstly, the leaf reflectance and transmittance were simulated using the leaf biophysical variables (i.e., chlorophyll content (Cab), carotenoid content(Car), dry matter content (Cm), water content (CW), structure parameter (N)) with PROSPECT-5 model. Then leaf reflectance and transmittance with average leaf inclination angle (ALA), soil coefficient (Psoil), solar zenith angle (SZA) and LAI were put into the SAIL model to simulate the canopy reflectance (Supplementary Materials, Table S1). Next, the simulated results of PROSAIL model combined with the Extended Fourier Amplitude Sensitivity Test (EFAST) method were used to evaluate the relative contributions of leaf and canopy parameters to the VIs in constructing the LAI seasonal trajectory. This method divides the contribution of variables into two sets, the first order indices give the contribution of individual variable, and the total order indices give the contribution of the interaction between variables (Saltelli et al., 2008). 2500 samples were randomly generated using EFAST for analysis (Supplementary Materials, Table S1).

3. Results

3.1. Seasonal trajectories of LAI and VI

Asymmetric seasonal trajectories of LAI were observed in most sites. The seasonal changes were distinct at deciduous forest and crop sites, while they were not obvious at some evergreen forest sites and no seasonal patterns at some other evergreen forest sites (Fig. 1(I)–(III)). At deciduous forest sites (Fig. 1(I)), the SGS occurred between April and May, and the EGS occurred between October and November. At crop sites (Fig. 1(III)), SGS occurred between May and June, and EGS occurred between September and October.

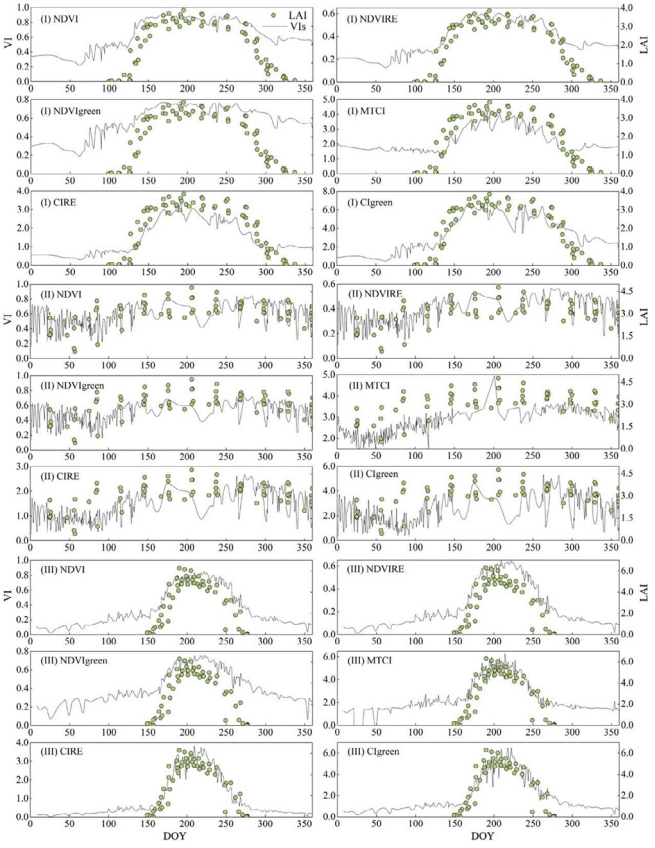

Fig. 1. Seasonal trajectories of LAI and VIs at the deciduous forest site: US-Ha1-EMS (I), evergreen forest site: CN-XSBN2 (II) and crop site: US-ne1 (III).

The seasonal trajectories of MERIS VIs were generally consistent with those of LAI. Especially the seasonal trajectories of CIRE at

Table 2
The spectral vegetation indices used in the study.

Index	Formulation	Reference
Normalized difference vegetation index (NDVI)		Rouse et al. (1974)
Red edge normalized difference vegetation index (NDVIRE)		Gitelson and Merzlyak (1994); Kross et al. (2015)
Green normalized difference vegetation index (NDVIgreen)		Gitelson et al. (1996); Nguy-Robertson et al. (2012)
MERIS terrestrial chlorophyll index (MTCI)		Dash and Curran (2004); Nguy-Robertson et al. (2012)
Red edge chlorophyll index (CIRE)		Gitelson (2005); Gitelson et al. (2003a,b); Heiskanen et al. (2013)
Green chlorophyll index (CIgreen)		Gitelson (2005); Gitelson et al. (2003a,b); Heiskanen et al. (2013)

deciduous forest and crop sites were the most consistent with that of LAI. Although similar seasonal trajectories were observed between MERIS VIs and LAI, the seasonal pattern was more clearly resolved by LAI than by MERIS VIs, and the temporal profiles of MERIS VIs and LAI were subject to substantial differences in width. For the SGS, increases in VI occurred earlier than those in LAI. Conversely, for the EGS, the decreases of LAI occurred earlier than those of VI. Thus, the length of the growing season (LGS) calculated using VI was longer than that using LAI. These differences were especially apparent for the deciduous forest sites. In addition, the decreases of the peak values in LAI occurred earlier than those in VI, with more obvious differences for NDVIgreen and NDVI than other VIs (Fig. 1).

3.2. Performances of VIs in constructing the LAI seasonal trajectory

3.2.1. Performances of VIs in constructing LAI seasonal trajectory for each site

The VIs at deciduous forest (i.e., US_Ha1_EMS, US_Ha1_LPH, US_UMB, US_MMS, JP_TKY and CA_Oas) and crop sites (i.e., US_ne1, US_ne2 and US_ne3) showed strong relationships with LAI, while the VIs at evergreen forest sites (i.e., CN_XSBN1, CN_XSBN2, CN_XSBN3, CN_XSBN4, CN_HT1 and CN_HT2) showed weak relationships with LAI (Fig. 2). But RMSE values for the LAI-VI relationships in evergreen forests sites are comparable to those for the LAI-VI relationships in deciduous forest and crop sites, because there is little differences among the LAI values in evergreen forest sites, leading to a low RMSE for LAI-VI relationships. For all sites, CIRE and NDVIRE fitted best to the LAI values, with a rank of mean R^2 by CIRE > NDVIRE > NDVI > MTCI > CIgreen > NDVIgreen (Fig. 3). Overall, the VI_{RE} (i.e., CIRE, NDVIRE and MTCI) had better performances than other VIs in site-level LAI-VI regressions.

3.2.2. Performances of VIs in constructing LAI seasonal trajectory for different vegetation types

All the six VIs had significant relationships with LAI for all vegetation types (Fig. 4). For deciduous forests, NDVIRE fitted best to LAI in the linear regressions, with a rank of R^2 by NDVIRE > NDVI > CIRE > CIgreen > NDVIgreen > MTCI, while for the quadratic polynomial regressions, CIRE fitted best to LAI, with a rank of R^2 by CIRE > NDVI > NDVIRE > CIgreen > NDVIgreen > MTCI. For evergreen forests, there were no significant differences among the performances of six VIs. NDVIRE had a slightly better performance than other VIs in the linear regressions, while CIRE had a slightly better performance than other VIs in the quadratic polynomial regressions. For crops, NDVIRE fitted best to LAI in the linear LAI-VI regressions, with a rank of R^2 by NDVIRE > CIRE > MTCI > NDVI > NDVIgreen > CIgreen, while for the quadratic polynomial LAI-VI regressions, CIRE fitted best to LAI, with a rank of R^2 by CIRE > NDVIRE > MTCI > NDVI > CIgreen > NDVIgreen (Fig. 4). In short, the quadratic polynomial regressions showed better results than the linear regressions.

3.2.3. Sensitivities of VIs to LAI seasonal variations

The sensitivities of six VIs to LAI variations in different vegetation types were quite different (Fig. 5). For deciduous forests, the NDVI exhibited the lowest values at LAI < 2, indicating the highest sensitivity; the NDVIRE had the highest sensitivity at LAI > 2; the CIRE, CIgreen and NDVIgreen exhibited higher sensitivities than NDVI when LAI > 3; and the MTCI exhibited higher sensitivity than NDVI when LAI > 4. For evergreen forests, there were no obvious differences among the sensitivities of six VIs to LAI when LAI < 5; and the CIRE and CIgreen had the highest sensitivities when LAI > 5, followed by MTCI, NDVIRE, NDVIgreen and NDVI. For crops, the sensitivities of all the VIs were similar at LAI < 3; and CIRE and MTCI had the highest sensitivities when LAI > 3, followed by CIgreen, NDVIRE, NDVIgreen and NDVI.

3.3. Effects of interfering factors on the construction of LAI seasonal trajectory with various VIs

3.3.1. The contributions of factors responsible for the variations of canopy reflectance

The contributions of canopy biophysical and non-canopy variables to different bands reflectance were quite different (Fig. 6). Psoil contributed most (> 40%) to the variations of green, red, red-edge and NIR bands reflectance at LAI < 1.0, but its contribution decreased with LAI. The green and RE bands reflectance were most affected by Cab (RE band: ~60% and green band: ~75%) at LAI > 1.0. Although the contributions of ALA and N increased with LAI when LAI > 2.0, Cab was still the greatest impact factor for green and RE bands reflectance, followed by ALA and N. The contributions of ALA (~10%) and N (~10%) to green band reflectance was obviously less than that to RE band (ALA: ~20% and N: ~20%), and they increased faster at relatively low LAI values. The red band reflectance was most affected by ALA when LAI > 1.0 (~60%). However, the contribution of ALA decreased with LAI, and the contribution of Cab gradually increased, replacing ALA as the greatest impact factor (~25%) for red band reflectance. Besides, the interaction between variables was also a significant impact factor for red band reflectance. The NIR band reflectance was most affected by ALA when LAI > 1.0 (~65%). When LAI > 2.0, the contribution of Cm increased rapidly with LAI, however, ALA still had the greatest contribution to NIR band reflectance, followed by Cm (~30%) and N (~7%).

Site name	R^2						RMSE					
US_Ha1_EMS	0.841***	0.880***	0.833***	0.736***	0.899***	0.833***	0.531	0.446	0.544	0.683	0.423	0.544
US_Ha1_LPH	0.829***	0.858***	0.803***	0.636***	0.861***	0.826***	0.568	0.517	0.610	0.828	0.511	0.573
US_UMB	0.913***	0.937***	0.885***	0.800***	0.923***	0.882***	0.236	0.201	0.272	0.359	0.222	0.275
US_MMS	0.790***	0.834***	0.839***	0.792***	0.835***	0.843***	0.633	0.563	0.553	0.631	0.562	0.548
CA_Oas	0.787***	0.813***	0.581***	0.603***	0.772***	0.614***	0.774	0.724	1.085	1.055	0.799	1.041
JP_TKY	0.726***	0.764***	0.546***	0.719***	0.740***	0.564***	0.379	0.354	0.492	0.390	0.373	0.482
CN_XSBN1	0.116*	0.212***	0.162***	0.177***	0.217***	0.165***	0.591	0.558	0.576	0.570	0.556	0.574
CN_XSBN2	0.312***	0.459***	0.231***	0.553***	0.457***	0.227***	0.742	0.658	0.786	0.598	0.659	0.787
CN_XSBN3	0.326***	0.438***	0.300***	0.484***	0.443***	0.313***	0.697	0.636	0.710	0.610	0.633	0.706
CN_XSBN4	0.125*	0.196**	0.119*	0.271***	0.204***	0.123*	0.801	0.768	0.804	0.732	0.764	0.802
CN_HT1	0.125	0.179*	0.126	0.123	0.185*	0.112	0.394	0.372	0.394	0.425	0.365	0.411
CN_HT2	0.241**	0.270**	0.227**	0.012	0.282**	0.226**	0.290	0.271	0.293	0.315	0.268	0.293
US_ne1	0.855***	0.892***	0.815***	0.874***	0.908***	0.832***	0.817	0.706	0.923	0.762	0.650	0.881
US_ne2	0.862***	0.910***	0.840***	0.869***	0.931***	0.867***	0.782	0.633	0.842	0.762	0.553	0.768
US_ne3	0.790***	0.879***	0.800***	0.839***	0.895***	0.807***	0.776	0.588	0.756	0.678	0.550	0.744
	NDVI	NDVIRE	NDVIgreen	MTCI	CIRE	CIgreen	NDVI	NDVIRE	NDVIgreen	MTCI	CIRE	CIgreen

Fig. 2. Statistical results of the LAI-VI regressions in each site. The color scale of chart represents different values of the R^2 and RMSE (red: high values, white: medium values, green: low values). *p < 0.05; **p < 0.01; ***p < 0.001.

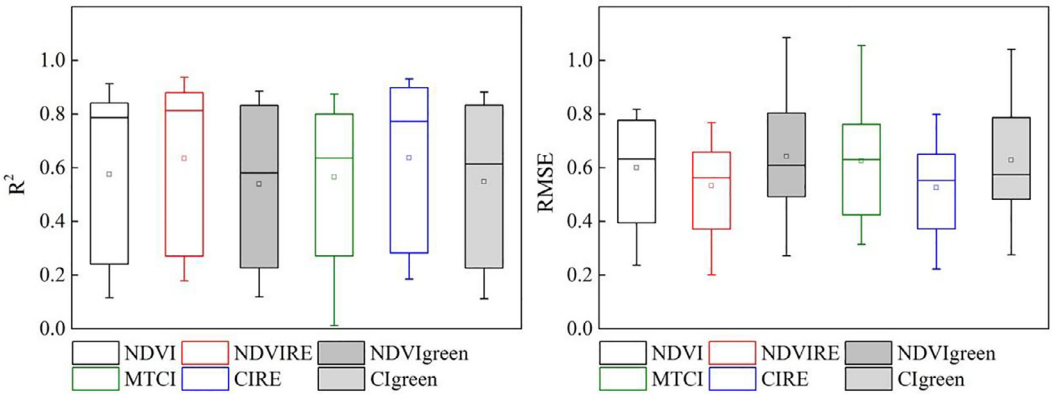

Fig. 3. Statistical results of the LAI-VI regressions at the sites. Two ends of the boxes represent the 25th and 75th percentiles; the bands in the box correspond to the median value; the ends of the whiskers indicate the lowest/highest value; and the open square denotes the mean value.

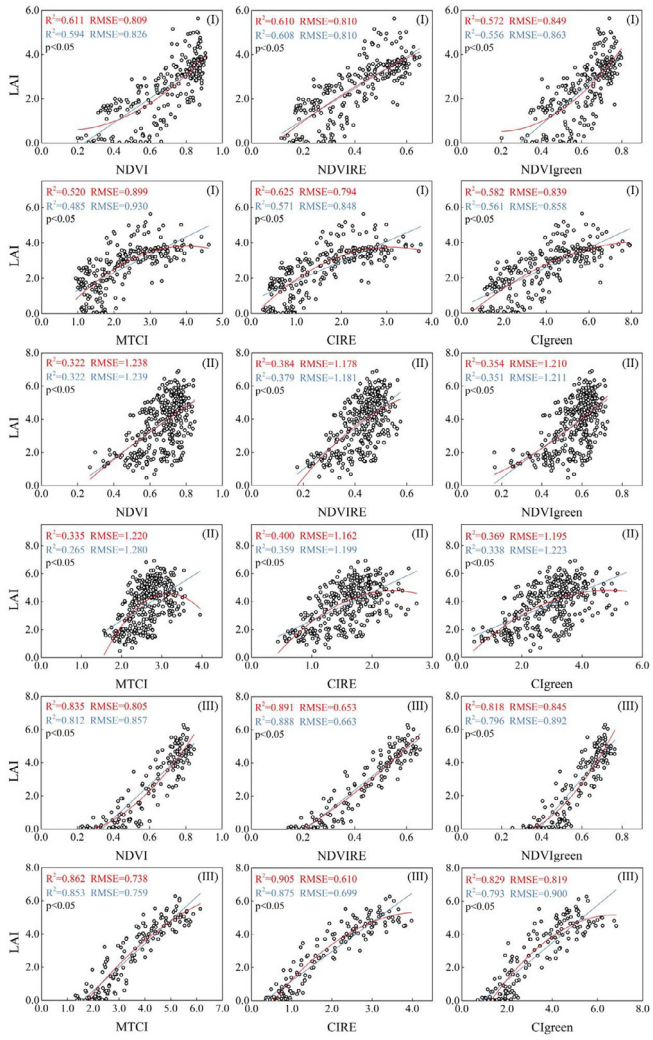

Fig. 4. The LAI-VI relationships for deciduous forests (I), evergreen forests (II) and crops (III). The blue and red lines are the linear and quadratic polynomial fitting LAI-VI relationships, respectively.

3.3.2. The contributions of factors responsible for the variations of vegetation indices

The contributions of canopy biophysical and non-canopy variables to different VIs differed a lot (Fig. 7). NDVI was most affected by ALA (> 30%), and followed by Cab. Although the contribution of ALA decreased, and that of Cab gradually increased with LAI, ALA still had a much greater contribution to NDVI than Cab. The contribution of ALA to NDVI was about 30% when LAI = 8. Except for NDVI, Cab had the greatest impact on other VIs, and its contribution was about 70%. In particularly for MTCI, the contribution of Cab could reach 90%. These VIs were also sensitive to ALA, but the contribution of ALA gradually decreased with LAI. Besides, N and Cm also had great impacts on VIs, and their contributions ranged between 5% and 10%. In addition, except for MTCI, other VIs were all affected by Psoil to different extent when LAI < 1.0.

4. Discussion

4.1. Application conditions and impact factors for various VIs in constructing the LAI seasonal trajectory

Six VIs were all closely related to LAI, and exhibited similar seasonal trajectories to LAI. Previous studies also confirmed that various VIs showed significant relationships with LAI in various vegetation types, including deciduous forests, boreal forests, mixed forests, crops and grasslands. In addition, both LAI and VIs had clear seasonal variations (Heiskanen et al., 2013; Heiskanen et al., 2012; Potithep et al., 2013; Tillack et al., 2014). However, some inconsistencies were also observed between the trajectories of LAI and VIs. At the SGS, increases in VI occurred earlier than those in LAI. Conversely, at the EGS, the minimum values of LAI occurred earlier than those of VI. This is mainly because LAI only reflects the information contained in the upper layers of vegetation, while VI reflects the mixed spectral information of canopy and understory vegetation, especially at the SGS and EGS periods (Nagai et al., 2010; Tillack et al., 2014). Thus, these differences are greater for VIs because VIs are susceptible to the influences of background information and soils.

The sensitivities of six VIs to LAI differed a lot over different ranges of LAI. For deciduous forests, NDVI had the highest sensitivity to LAI when LAI < 2, while NDVIRE had the highest sensitivity when LAI > 2. For crops, all the VIs had the similar sensitivities at LAI < 3, while CIRE and MTCI were most sensitive to LAI variations at LAI > 3. Viña et al. (2011) and Nguy-Robertson et al. (2012) also demonstrated that different VIs had different sensitivities to LAI for two crops (i.e., maize and soybean), and there were also great differences in the performances of various VIs in LAI estimation. Thus, the optimal VIs over different ranges of LAI are suggested to estimate LAI.

Tillack et al. (2014) pointed out that the construction of LAI trajectory with VIs was affected by diverse factors, such as growth period, vegetation composition, tree age, and background reflectance. Most VIs did not always have stable performances, when they are applied to constructing LAI seasonal trajectory for different vegetation types with various canopy and leaf structures. From the point view of radiative transfer, the construction of LAI seasonal trajectory using VIs is mainly

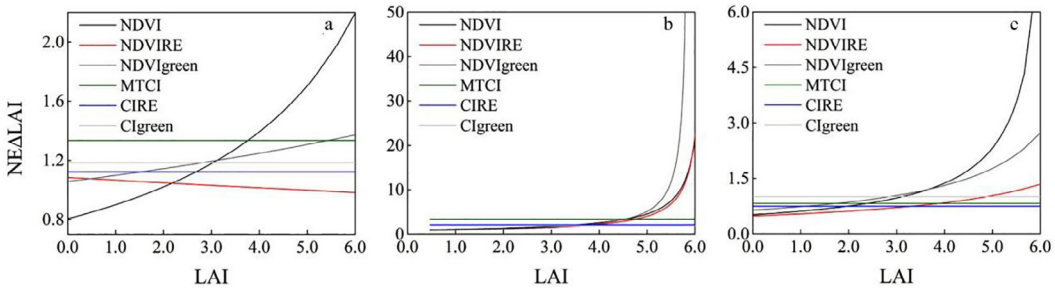

Fig. 5. The sensitivities of VIs to LAI variations for deciduous forests (a), evergreen forests (b) and crops (c).

affected by leaf properties (e.g., chlorophyll content, water content and dry matter content), canopy structures (e.g., leaf inclination angle distribution and clumping index), soil background reflectance, sun-sensor geometry and illumination conditions (Jacquemoud et al., 2009; Liu et al., 2012; Xie et al., 2018). A quantitative analysis was conducted for these impact factors in this study, and we found that Cab had the greatest contribution to the variations of VIs (except for NDVI), followed by ALA. NDVI was most affected by ALA and also greatly affected by Cab. In addition, N and Cm were also important factors influencing the variations of VIs. In the ranges of low LAI values, Psoil had a relative greater contribution to VIs. The results are highly consistent with many previous studies, in which they declared that VI is a complex indicator affected by many factors, and Cab and ALA were the main contributors, and the contributions of other factors were relatively weak (Dong et al., 2019; Liu et al., 2012; Xie et al., 2018).

4.2. Potential advantages and impact factors for VI_{RE} in constructing LAI seasonal trajectory

Green, red and RE bands are all sensitive to the vegetation information, however, the VIs constructed by RE bands are more effective in LAI estimation than that by other spectral bands, and can significantly improve the accuracy of LAI estimation (TIan et al., 2017; Korhonen et al., 2017; Nguy-Robertson and Gitelson, 2015). We also found that no matter in the construction of LAI seasonal trajectory at

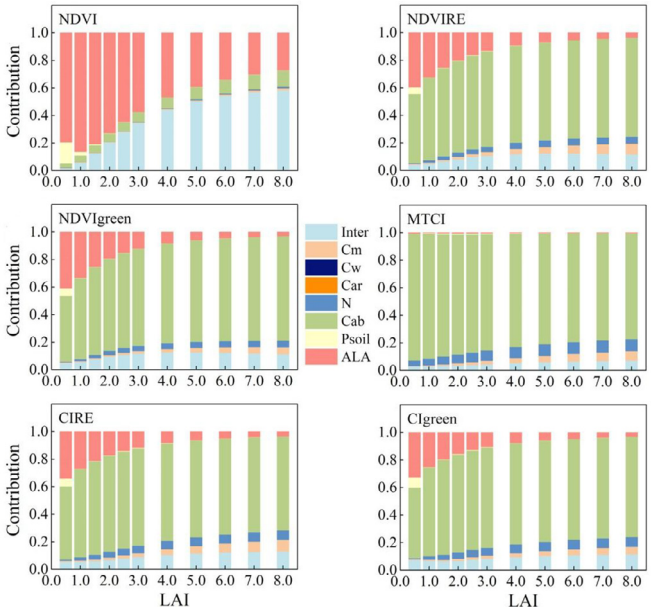

Fig. 7. Contributions of canopy biophysical and non-canopy variables responsible for the variations of vegetation indices.

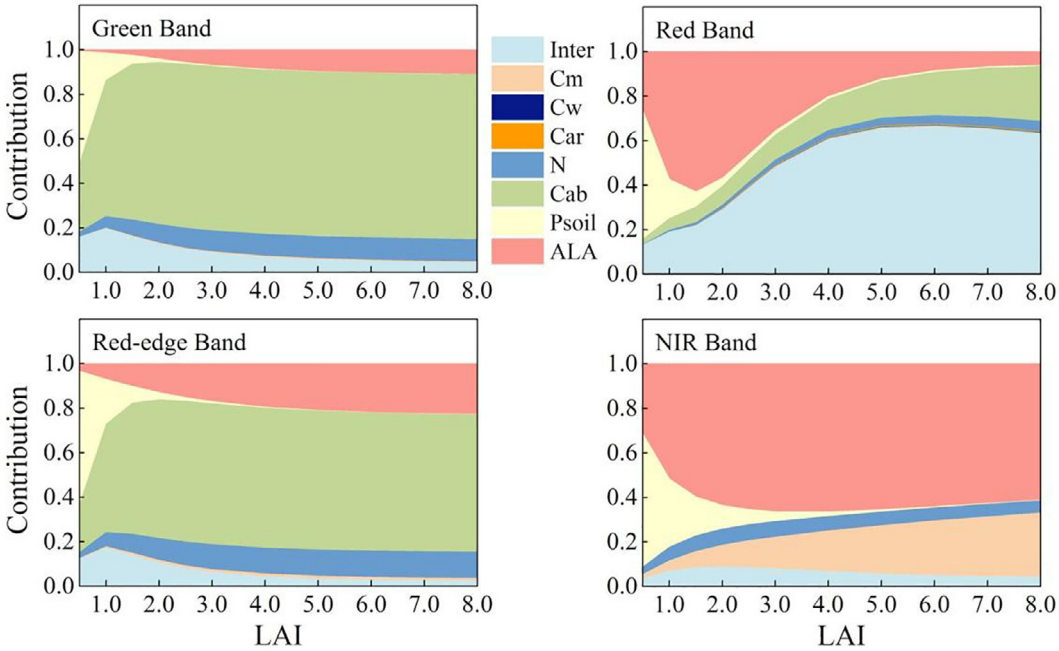

Fig. 6. Contributions of canopy biophysical and non-canopy variables responsible for the variations of spectral reflectance; "Inter" represents the contribution of the interaction between variables.

the sites or for different vegetation types, VI_{RE} (i.e., CIRE and NDVIRE) performed more stable and better than other VIs in the construction of LAI seasonal trajectory. Moreover, the VI_{RE} maintained relatively high sensitive to LAI over the whole range of LAI, and were effective in partly overcoming the saturation problem at high LAI values. These results are highly agreement with those of previous studies; they found the VI_{RE} can give a quick response to the small variations of spectral reflectance, environmental stress and LAI (Delegido et al., 2011; Schuster et al., 2012; Viña et al., 2011). This is because the RE band is at the wavelength between red and NIR bands and there has a sharp variation in vegetation spectral reflectance, characterizing the transition from strong absorption of chlorophyll to cellular scattering (Delegido et al., 2013; Hatfield et al., 2008; Nguy-Robertson et al., 2012).

Using GSA, we found that the VI_{RE} was greatly affected by Cab and ALA. However, the contribution of ALA decreased with LAI, especially for when the canopy is quite dense and the canopy transmittance is low (LAI $>$ 2). Thus, the LAI-VI relationship was mainly controlled by Cab But in fact, the dynamic range of Cab in vegetation is relative narrow (Dong et al., 2019; Féret et al., 2011), besides, the influence of other factors (e.g., ALA and N) on VI_{RE} were relatively weak. Thus, the VI_{RE} had the potential to establish a universal model to estimate LAI for crops or forests with different canopy structures. The results were consistent with previous studies. Nguy-Robertson et al. (2014) revealed the red edge constructed VIs were promising for establishing a universal algorithm for LAI estimation in four crops including maize, soybean, wheat and potato. Dong et al. (2019) also found similar results that a universal model for estimating LAI can be developed using the red edge constructed VIs derived from RapideEye data for crops. Although the VI_{RE} performed better in constructing LAI seasonal trajectory for deciduous forests and crops, their advantages in LAI estimation for evergreen forests were not obvious. This may be due to the unapparent seasonality of evergreen forests, so that the weak seasonal signals are not easily captured by MREIS due to the compounding influences of atmosphere, BRDF and shadows (Brown et al., 2017).

4.3. Application prospects and uncertainties

We found that the VI_{RE} were more sensitive to LAI variations than other VIs. Besides, they had the potential to develop a universal model for estimating LAI in forests or crops with different canopy structures. The results further demonstrate a great potential of VI_{RE} in crop growth monitoring, ecological model simulation and biomass estimation, as previous studies have proved (Bobée et al., 2012; Claverie et al., 2012; Richardson et al., 2011; Shang et al., 2014). Recently, more and more high-resolution remote sensing data with RE band are available, such as Sentinel-2 and GF-6. These satellite sensors with RE band are expected to provide high-accuracy LAI products for environmental, agricultural and forestry applications.

Although many factors affected the construction of LAI seasonal trajectory with VIs were discussed in this study, there still some other aspects are not considered, such as the measurement methods and sampling strategies of LAI data, they are key issues for obtaining LAI observed data accurately, and may be different at each site, which will bring uncertainties to our analysis. In addition, the LAI-VI relationships for three vegetation types were discussed in the study, however, the number of sites for each vegetation type is limited, and the influences of meteorological factors on the construction of LAI seasonal trajectory with VIs were ignored. But the meteorological factors such as temperature, precipitation and photoperiod have significant influence on vegetation growth (Buyantuyev and Wu, 2012; Hu et al., 2011), and most biological processes of vegetation can be explained by the variations of meteorological factors (Jolly et al., 2005; Zhang et al., 2012). In the future, more observed data will be available for the study with the development of data sharing policies and information technology, thus, the meteorological data should be considered in the construction of LAI seasonal trajectory with VIs. In addition, the findings of this study should also be tested in more sites for different vegetation types in various climate zones, to further improve the accuracy of LAI seasonal estimation.

5. Conclusions

The performances of six vegetation indices (VIs) (i.e., Normalized difference vegetation index (NDVI), Red edge normalized difference vegetation index (NDVIRE), Green normalized difference vegetation index (NDVIgreen), MERIS terrestrial chlorophyll index (MTCI), Red edge chlorophyll index (CIRE) and Green chlorophyll index (CIgreen)) in constructing LAI seasonal trajectory for deciduous forests, evergreen forests and crops were evaluated in this study. Besides, we also quantitatively analyzed the various factors which may affect the construction of LAI seasonal trajectory using VIs. There were great differences in the performances of six VIs in constructing LAI seasonal trajectory. The sensitivities of various VIs to LAI also differed over different ranges of LAI. The VIs constructed by the red edge band (VI_{RE}) maintained relatively high sensitivity to LAI over the whole range of LAI, showing advantages in constructing LAI seasonal trajectory. Moreover, VI_{RE} had the potential to develop a universal model for estimating LAI. From the radiative transfer prospective, chlorophyll content (Cab) and Average leaf inclination angle (ALA) had the greatest impacts on VIs. NDVI was most affected by ALA, and other VIs were most affected by Cab. Besides, structure parameter (N) and dry matter content (Cm) also had great impacts on VIs, and all the VIs at low values were affected by Psoil to different extent.

In summary, the optimal VI over different ranges of LAI is suggested to estimate LAI for different vegetation types. In addition, the VI_{RE} should be a preferred choice for estimating LAI to reduce the simulation errors of seasonal LAI, if the RE band is available.

CRediT authorship contribution statement

Kun Qiao: Conceptualization, Formal analysis, Methodology, Writing - original draft, Writing - review & editing. **Wenquan Zhu:** Conceptualization, Methodology, Writing - review & editing. **Zhiying Xie:** Writing - review & editing, Visualization.

Declaration of Competing Interest

The authors declare that they have no known competing financial interests or personal relationships that could have appeared to influence the work reported in this paper.

Acknowledgements

This research was supported by the National Natural Science Foundation of China (Grant No. 41771047) and the State Key Laboratory of Earth Surface Processes and Resource Ecology (Grant No. 2017-FX-01(1)).

Appendix A. Supplementary data

Supplementary data to this article can be found online at https://doi.org/10.1016/j.ecolind.2020.106153.

References

Atzberger, C., Darvishzadeh, R., Immitzer, M., Schlerf, M., Skidmore, A., le Maire, G., 2015. Comparative analysis of different retrieval methods for mapping grassland leaf area index using airborne imaging spectroscopy. Int. J. Appl. Earth Observ. Geoinf. 43, 19–31.

Battaglia, M., Sands, P., White, D., Mummery, D., 2004. CABALA: a linked carbon, water and nitrogen model of forest growth for silvicultural decision support. For. Ecol. Manage. 193, 251–282.

Birky, A.K., 2001. NDVI and a simple model of deciduous forest seasonal dynamics. Ecol. Model. 143, 43–58.
Bobée, C., Ottlé, C., Maignan, F., de Noblet-Ducoudré, N., Maugis, P., Lézine, A.M., Ndiaye, M., 2012. Analysis of vegetation seasonality in Sahelian environments using MODIS LAI, in association with land cover and rainfall. J. Arid Environ. 84, 38–50.
Brown, L.A., Dash, J., Ogutu, B.O., Richardson, A.D., 2017. On the relationship between continuous measures of canopy greenness derived using near-surface remote sensing and satellite-derived vegetation products. Agric. For. Meteorol. 247, 280–292.
Buyantuyev, A., Wu, J., 2012. Urbanization diversifies land surface phenology in arid environments: interactions among vegetation, climatic variation, and land use pattern in the Phoenix metropolitan region, USA. Landscape Urban Plann. 105, 149–159.
Campos-Taberner, M., García-Haro, F.J., Camps-Valls, G., Grau-Muedra, G., Nutini, F., Crema, A., Boschetti, M., 2016. Multitemporal and multiresolution leaf area index retrieval for operational local rice crop monitoring. Remote Sens. Environ. 187, 102–118.
Casa, R., Varella, H., Buis, S., Guérif, M., De Solan, B., Baret, F., 2012. Forcing a wheat crop model with LAI data to access agronomic variables: evaluation of the impact of model and LAI uncertainties and comparison with an empirical approach. Eur. J. Agron. 37, 1–10.
Chen, J.M., Black, T.A., 1992. Foliage area and architecture of plant canopies from sunfleck size distributions. Agric. For. Meteorol. 60, 249–266.
Cheng, Q., Huang, J., Wang, R., Tang, Y., 2003. Analyses of the correlation between rice LAI and simulated MODIS vegetation indices, red edge position. Trans. CSAE 19, 104–107.
Claverie, M., Demarez, V., Duchemin, B., Hagolle, O., Ducrot, D., Marais-Sicre, C., Dejoux, J.-F., Huc, M., Keravec, P., Béziat, P., Fieuzal, R., Ceschia, E., Dedieu, G., 2012. Maize and sunflower biomass estimation in southwest France using high spatial and temporal resolution remote sensing data. Remote Sens. Environ. 124, 844–857.
Dash, J., Curran, P.J., 2004. The MERIS terrestrial chlorophyll index. Int. J. Remote Sens. 25, 5403–5413.
Delegido, J., Verrelst, J., Alonso, L., Moreno, J., 2011. Evaluation of Sentinel-2 red-edge bands for empirical estimation of green LAI and chlorophyll content. Sensors (Basel) 11, 7063–7081.
Delegido, J., Verrelst, J., Meza, C.M., Rivera, J.P., Alonso, L., Moreno, J., 2013. A red-edge spectral index for remote sensing estimation of green LAI over agroecosystems. Eur. J. Agron. 46, 42–52.
Din, M., Zheng, W., Rashid, M., Wang, S., Shi, Z., 2017. Evaluating hyperspectral vegetation indices for leaf area index estimation of Oryza sativa L. at diverse phenological stages. Front. Plant Sci. 8, 820.
Dong, T., Liu, J., Shang, J., Qian, B., Ma, B., Kovacs, J.M., Walters, D., Jiao, X., Geng, X., Shi, Y., 2019. Assessment of red-edge vegetation indices for crop leaf area index estimation. Remote Sens. Environ. 222, 133–143.
Eitel, J.U.H., Vierling, L.A., Litvak, M.E., Long, D.S., Schulthess, U., Ager, A.A., Krofcheck, D.J., Stoscheck, L., 2011. Broadband, red-edge information from satellites improves early stress detection in a New Mexico conifer woodland. Remote Sens. Environ. 115, 3640–3646.
Féret, J.-B., François, C., Gitelson, A., Asner, G.P., Barry, K.M., Panigada, C., Richardson, A.D., Jacquemoud, S., 2011. Optimizing spectral indices and chemometric analysis of leaf chemical properties using radiative transfer modeling. Remote Sens. Environ. 115, 2742–2750.
Garrigues, S., Lacaze, R., Baret, F., Morisette, J.T., Weiss, M., Nickeson, J.E., Fernandes, R., Plummer, S., Shabanov, N.V., Myneni, R.B., Knyazikhin, Y., Yang, W., 2008. Validation and intercomparison of global Leaf Area Index products derived from remote sensing data. J. Geophys. Res. Biogeosci. 113, 1–20.
Gitelson, A.A., 2005. Remote estimation of canopy chlorophyll content in crops. Geophys. Res. Lett. 32, L08403.
Gitelson, A.A., Kaufman, Y.J., Merzlyak, M.N., 1996. Use of a green channel inremote sensing of global vegetation from EOS-MODIS. Remote Sens. Environ. 58, 289–298.
Gitelson, A.A., Viña, A., Arkebauer, T.J., Rundquist, D.C., Keydan, G., Leavitt, B., 2003b. Remote estimation of leaf area index and green leaf biomass in maize canopies. Geophys. Res. Lett. 30, 1248.
Gitelson, A.A., Merzlyak, M.N., 1994. Spectral reflectance changes associated with-autumn senescence of Aesculus hippocastanum L. and Acer platanoides L. Leaves. Spectral features and relation to chlorophyll estimation. J. Plant Physiol. 143, 286–292.
Gitelson, A.A., Gritz, Y., Merzlyak, M.N., 2003a. Relationships between leaf chlorophyll content and spectral reflectance and algorithms for non-destructive chlorophyll assessment in higher plant leaves. J. Plant Physiol. 160, 271–282.
Gu, Y., Wylie, B.K., Howard, D.M., Phuyal, K.P., Ji, L., 2013. NDVI saturation adjustment: a new approach for improving cropland performance estimates in the Greater Platte River Basin, USA. Ecol. Indic. 30, 1–6.
Hatfield, J.L., Gitelson, A.A., Schepers, J.S., Walthall, C.L., 2008. Application of spectral remote sensing for agronomic decisions. Agron. J. 100, 117–131.
Heiskanen, J., Rautiainen, M., Stenberg, P., Mõttus, M., Vesanto, V.-H., Korhonen, L., Majasalmi, T., 2012. Seasonal variation in MODIS LAI for a boreal forest area in Finland. Remote Sens. Environ. 126, 104–115.
Heiskanen, J., Rautiainen, M., Stenberg, P., Mõttus, M., Vesanto, V.-H., 2013. Sensitivity of narrowband vegetation indices to boreal forest LAI, reflectance seasonality and species composition. ISPRS J. Photogramm. Remote Sens. 78, 1–14.
Hu, M.Q., Mao, F., Sun, H., Hou, Y.Y., 2011. Study of normalized difference vegetation index variation and its correlation with climate factors in the three-river-source region. Int. J. Appl. Earth Obs. Geoinf. 13, 24–33.
Jacquemoud, S., Verhoef, W., Baret, F., Bacour, C., Zarco-Tejada, P.J., Asner, G.P., François, C., Ustin, S.L., 2009. PROSPECT + SAIL models: a review of use for vegetation characterization. Remote Sens. Environ. 113, S56–S66.
Jolly, W.M., Nemani, R., Running, S.W., 2005. A generalized, bioclimatic index to predict foliar phenology in response to climate. Global Change Biol. 11, 619–632.
Korhonen, L., Hadi, Packalen, P., Rautiainen, M., 2017. Comparison of Sentinel-2 and Landsat 8 in the estimation of boreal forest canopy cover and leaf area index. Remote Sens. Environ. 195, 259–274.
Kross, A., McNairn, H., Lapen, D., Sunohara, M., Champagne, C., 2015. Assessment of RapidEye vegetation indices for estimation of leaf area index and biomass in corn and soybean crops. Int. J. Appl. Earth Obs. Geoinf. 34, 235–248.
le Maire, G., Marsden, C., Nouvellon, Y., Grinand, C., Hakamada, R., Stape, J.-L., Laclau, J.-P., 2011. MODIS NDVI time-series allow the monitoring of Eucalyptus plantation biomass. Remote Sens. Environ. 115, 2613–2625.
Li, X., Zhang, Y., Luo, J., Jin, X., Xu, Y., Yang, W., 2016. Quantification winter wheat LAI with HJ-1CCD image features over multiple growing seasons. Int. J. Appl. Earth Obs. Geoinf. 44, 104–112.
Liu, J., Pattey, E., Jégo, G., 2012. Assessment of vegetation indices for regional crop green LAI estimation from Landsat images over multiple growing seasons. Remote Sens. Environ. 123, 347–358.
Moulin, S., 1999. Impacts of model parameter uncertainties on crop reflectance estimates: a regional case study on wheat. Int. J. Remote Sens. 20, 213–218.
Nagai, S., Nasahara, K.N., Muraoka, H., Akiyama, T., Tsuchida, S., 2010. Field experiments to test the use of the normalized-difference vegetation index for phenology detection. Agric. For. Meteorol. 150, 152–160.
Nguy-Robertson, A., Gitelson, A., Peng, Y., Viña, A., Arkebauer, T., Rundquist, D., 2012. Green leaf area index estimation in maize and soybean: combining vegetation indices to achieve maximal sensitivity. Agron. J. 104, 1336–1347.
Nguy-Robertson, A.L., Gitelson, A.A., 2015. Algorithms for estimating green leaf area index in C3 and C4 crops for MODIS, Landsat TM/ETM + , MERIS, Sentinel MSI/OLCI, and Venμs sensors. Remote Sens. Lett. 6, 360–369.
Nguy-Robertson, A.L., Peng, Y., Gitelson, A.A., Arkebauer, T.J., Pimstein, A., Herrmann, I., Karnieli, A., Rundquist, D.C., Bonfil, D.J., 2014. Estimating green LAI in four crops: potential of determining optimal spectral bands for a universal algorithm. Agric. For. Meteorol. 192–193, 140–148.
Potithep, S., Nagai, S., Nasahara, K.N., Muraoka, H., Suzuki, R., 2013. Two separate periods of the LAI–VIs relationships using in situ measurements in a deciduous broadleaf forest. Agric. For. Meteorol. 169, 148–155.
Richardson, A.D., Dail, D.B., Hollinger, D.Y., 2011. Leaf area index uncertainty estimates for model–data fusion applications. Agric. For. Meteorol. 151, 1287–1292.
Rouse Jr., J.W., Haas, R.H., Schell, J.A., Deering, D.W., 1974. Monitoring vegetation systems in the Great Plains with ERTS. In: Freden, S.C., Becker, M.A. (Eds.), Third ERTS Symposium. NASA (SP-351), pp. 309–317.
Saltelli, A., Ratto, M., Andres, T., Campolongo, F., Cariboni, J., Gatelli, D., Saisana, M., Tarantola, S., 2008. Global Sensitivity Analysis: The Primer. John Wiley & Sons.
Schuster, C., Förster, M., Kleinschmit, B., 2012. Testing the red edge channel for improving land-use classifications based on high-resolution multi-spectral satellite data. Int. J. Remote Sens. (17), 5583–5599.
Shang, J., Liu, J., Huffman, T., Qian, B., Pattey, E., Wang, J., Zhao, T., Geng, X., Kroetsch, D., Dong, T., Lantz, N., 2014. Estimating plant area index for monitoring crop growth dynamics using Landsat-8 and RapidEye images. J. Appl. Remote Sens. 8, 085196.
Tian, J., Wang, L., Li, X., Gong, H., Shi, C., Zhong, R., Liu, X., 2017. Comparison of UAV and WorldView-2 imagery for mapping leaf area index of mangrove forest. Int. J. Appl. Earth Obs. Geoinf. 61, 22–31.
Tillack, A., Clasen, A., Kleinschmit, B., Förster, M., 2014. Estimation of the seasonal leaf area index in an alluvial forest using high-resolution satellite-based vegetation indices. Remote Sens. Environ. 141, 52–63.
Viña, A., Gitelson, A.A., Nguy-Robertson, A.L., Peng, Y., 2011. Comparison of different vegetation indices for the remote assessment of green leaf area index of crops. Remote Sens. Environ. 115, 3468–3478.
Xie, Q., Dash, J., Huang, W., Peng, D., Qin, Q., Mortimer, H., Casa, R., Pignatti, S., Laneve, G., Pascucci, S., Dong, Y., Ye, H., 2018. Vegetation indices combining the red and red-edge spectral information for leaf area index retrieval. IEEE J. Sel. Top. Appl. Earth Obs. Remote Sens. 11, 1482–1493.
Xu, B., Li, J., Park, T., Liu, Q., Zeng, Y., Yin, G., Zhao, J., Fan, W., Yang, L., Knyazikhin, Y., Myneni, R.B., 2018. An integrated method for validating long-term leaf area index products using global networks of site-based measurements. Remote Sens. Environ. 209, 134–151.
Yan, G., Hu, R., Luo, J., Weiss, M., Jiang, H., Mu, X., Xie, D., Zhang, W., 2019. Review of indirect optical measurements of leaf area index: recent advances, challenges, and perspectives. Agric. For. Meteorol. 265, 390–411.
Zhang, Y., Qu, Y., Wang, J., Liang, S., Liu, Y., 2012. Estimating leaf area index from MODIS and surface meteorological data using a dynamic Bayesian network. Remote Sens. Environ. 127, 30–43.